

# High Voltage Boosting Converters Based on Bootstrap Capacitors

Aseeb P. P<sup>1</sup>, Nayas Qudrathulla P. P<sup>2</sup>

<sup>1</sup> MEA Engineering College, Perinthalmanna, India

<sup>2</sup> MEA Engineering College, Perinthalmanna, India

## Abstract

In this project, two high voltage-boosting converters are presented. By changing the connection position of the anode of the diode and by using different Pulse-Width-Modulation control strategies, different voltage conversion ratios can be obtained. These converters are constructed based on bootstrap capacitors and boost inductors. Above all, two boost inductors with different values, connected in series, can still make the proposed converters work appropriately. The proposed converter gives high efficiency, low output ripple and low cost. The proposed converter gives the output power 200 V DC from 24 V DC at power 100 W. The proposed converter gives a high efficiency and transformation ratio by reducing the conduction losses and switching losses. Simulation was done in MATLAB/Simulink and results were verified for open loop and closed loop of converter. Experimental prototype was designed for a lower output power and results were verified.

**Keywords:** *Bootstrap Capacitors, Boost Inductors, Voltage-Boosting Converter, Voltage Conversion Ratio.*

## 1. Introduction

To design, develop and validate a high voltage boosting converter. The project work consists of a review of some of the important power electronic converters which are already used for power conversion. This work proposing a new DC-DC converter with high step up ratio. Scope of this thesis is limited to the steady state analysis and characteristics of the proposed converter under continuous conduction mode.

Major contributions of the project are:

1. Proposing two new DC-DC converters giving high step-up ratio and conversion efficiency.

2. The converters consist of bootstrap capacitors and boost inductors, in order to obtain high voltage conversion ratio.

The background and motivation for this work is the emerging need for high power converters to boost voltage levels from low voltage electrical power sources to higher voltages required by the load. Fig.1.1, presents the typical power architecture of these systems.

Many conventional DC-DC converters are present, in which isolated converters are preferred because the non-isolated converters do not satisfy the requirements of galvanic isolation standards. In many DC-DC applications, multiple outputs are required and output isolation may need to be implemented depending on the application. In addition, input to output isolation may be required to meet safety specifications.

An isolated DC-DC converter boosts the unregulated low voltage supply to a much higher DC voltage, typically 400 V for single phase and 7-800 V for three phase utility grid interface. Wideinput voltage range, typically in the range of 30-60 V, is normally required. Subsequently, a DC-AC inverter will typically convert high voltage DC output into single- or threephase ac voltage for interface to the utility grid or control of electrical motors etc.

Since the DC-AC converter operates at high voltage and is well known from other high power applications such as in UPSs, motor drives, solar inverters etc., the objective of this study is to focus on achieving high efficiency in the critical low voltage to high voltage DC-DC converter.

Achieving higher conversion efficiency in the power electronic converter required for boosting the low source voltage to the higher voltage required by the application, will therefore become a major competitive parameter in these applications.

## 2. Literature Study

The various types of converter are buck converter, boost converter, buck-boost converter, Cuk-converter, SEPIC converter, full-bridge and half-bridge converter, boost converter with improved transfer ratio, push-pull converter, flyback converter, resonant converter, KY converter and its derivatives and so on. These converters can be classified based on various categories. These converters can be classified as isolated and non-isolated converters, unidirectional and bidirectional converters, step-up and step-down converters, single input and multi-input converters, Low power application and high power application converters etc.

A process that changes one DC voltage to a different DC voltage is called DC to DC conversion. A boost converter is a DC to DC converter with an output voltage greater than the source voltage. A boost converter is sometimes called a step-up converter since it “steps up” the source voltage. Power for the boost converter can come from any suitable DC sources, such as batteries, solar panels, rectifiers and DC generators.

Flyback converter is used in both AC-DC and DC-DC conversion with galvanic isolation between the input and any outputs. The flyback converter is a buck-boost converter with the inductor split to form a transformer, so that the voltage ratios are multiplied with an additional advantage of isolation. A flyback converter stores energy as a magnetic field in the inductor air gap during the time the converter switching element (transistor) is conducting. When the switch turns off, the stored magnetic field collapses and the energy is transferred to the output of the flyback converter as electric current.

*Boost Converter with Improved Transfer Ratio* by DV Nicolae<sup>1</sup>, CG Richards and JFJ van Rensburg [3] presents a variation of the classical boost converter with the aim of improving the boost factor. The general idea is to charge parallel the inductors and transfer serially to the output increasing the boost ratio. The influence of the losses is presented is concluded that this application is not effective for more than two inductors. The performances of this novel boost converter are validated via simulation and experimental model.

*A New High Step-Up Converter for UPS Applications* By Carlos E. A. Silva, Rene P. T. Bascope, Demercil S and Oliveira Jr. [11] proposes the use of a voltage doubler rectifier as the output stage of an interleaved boost converter with coupled inductors. The obtained voltage gain is twice that of traditional boost converters due to the doubler stage, as coupled inductors provide additional voltage gain, although voltage stress across the switches is not increased. The resulting topology is adequate for battery sourced systems which require low current ripple and high voltage gain e.g. UPS's and audio amplifiers. Additionally, it can be used to obtain symmetrical power supply.

*KY Converters and its Derivatives* by K. I. Hwu, Member, IEEE, and Y. T. Yau [15], a voltage-boosting converter, named KY converter (i.e., 1-plus- $D$  converter), is presented. Unlike the traditional non-isolated boost converter, this converter possesses fast load transient responses, which is similar to the buck converter with synchronous rectification. In addition, it possesses non-pulsating output current, there by not only decreasing the current stress on the output capacitor but also reducing the output voltage ripple. Besides, 1-plus- $2D$  and 2-plus- $D$  converters, derived from the KY converter, are presented based on the same structure but different pulse width-modulation control strategies. Above all, the main difference between the KY converter and its derivatives is that the latter ones possess higher output voltages than the former one under the same duty cycle.

Theoretically, conventional boost converters are able to achieve high step-up voltage gain in heavy duty load conditions. With a very high duty ratio, the output rectifier conducts for only a very short time during each switching cycle, thus resulting in serious reverse-recovery problems and an increase in the rating of the rectification diode. A boost converter including an inductor with a primary winding and secondary winding is able to produce higher output voltage with high conversion efficiency.

## 3. High Voltage Boosting Converters Based on Bootstrap Capacitors

This chapter gives a review of a high voltage DC-DC boosting converters based on bootstrap capacitors circuit with high voltage conversion ratio. These converters are constructed based on bootstrap capacitors and boost inductors. Above all, two boost inductors with different values, connected in series, can still make the high voltage converters work appropriately.

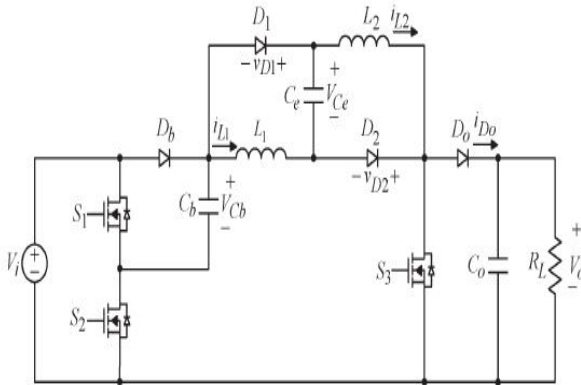


Fig.1 (a) High Voltage Type 1 Boosting Converter

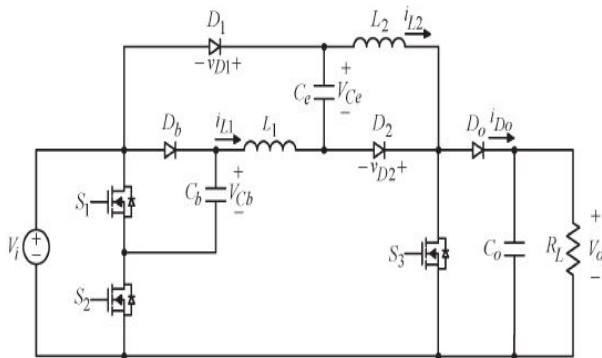


Fig.1 (b) High Voltage Type 2 Boosting Converter

The proposed two high voltage-boosting converters have individual voltage conversion ratios and individual pulse-width modulation (PWM) control strategies. Hence, the type 1 converter is described in Fig. 3.1 (a), whereas the type 2 converter is shown in Fig. 3.1 (b). It is noted that the difference in circuit between Fig.3.1 (a) and (b) is the location of the anode of  $D_1$ . Each converter contains three MOSFET switches  $S_1, S_2$ , and  $S_3$ , two bootstrap capacitors  $C_b$  and  $C_e$ , three bootstrap diodes  $D_b, D_1$ , and  $D_2$ , one output diode  $D_o$ , two inductors  $L_1$  and  $L_2$ , one output capacitor  $C_o$ , and

one output resistor  $R_L$ . In addition, the input voltage is signified by  $V_i$ , the output voltage is represented by  $V_o$ , the voltages across  $C_b, C_e, D_1$ , and  $D_2$  are shown by  $V_{Cb}, V_{Ce}, v_{D1}$ , and  $v_{D2}$ , respectively, and the currents flowing through  $L_1, L_2$  and  $D_o$  are denoted by  $i_{L1}, i_{L2}$ , and  $i_{D_o}$ , respectively.

It is noted that the proposed converters are based on the charge pump of the KY converter and the series boost converter. By doing so, the conversion ratios can be upgraded further. Above all, if the anode of the diode  $D_1$  is connected to the cathode of the diode  $D_b$ , the conversion voltage ratio in continuous conduction mode (CCM) is  $(3 + D)/(1 - D)$ , where  $D$  is the duty cycle of the PWM control signal created from the controller, whereas if the anode of the diode  $D_1$  is connected to the anode of the diode  $D_b$  with switch turn-on types different from those of the former, the conversion ratio in CCM is  $(3 - D)/(1 - D)$ . Therefore, the proposed converters can be used according to industrial applications.

For these two converters to be considered, the PWM turn on types for three switches and the voltages on the bootstrap capacitors are tabulated in Table I. Above all, the converters operated in the CCM and in the discontinuous conduction mode (DCM) are to be analysed in the following, under the condition that  $L_1$  is equal to  $L_2$ . However, actually,  $L_1$  is different from  $L_2$ . Consequently, for analysis convenience, types 1 and 2 operated only in CCM under the condition that  $L_1$  is larger than  $L_2$  or  $L_1$  is smaller than  $L_2$  are taken into account.

Before this section is taken up, some assumptions are given as follows: 1) the blanking times between the switches are omitted; 2) the voltage drops across the switches and diodes during the turn-on period are negligible; and 3) since the bootstrap capacitors  $C_b$  and  $C_e$ , operating based on the charge pump principle, are abruptly charged to some voltage within a very short time, which is much less than the switching period  $T_s$ , the values of  $C_b$  and  $C_e$  are large enough to keep the voltages across themselves constant at some values, and hence it is reasonable that the voltages across the capacitors  $C_b$  and  $C_e$  are  $V_i$  and  $2V_i$  for type 1, respectively, and the voltages across the capacitors  $C_b$  and  $C_e$  are both  $V_i$  for type 2.

### 3.1 Modes of Operations for Type 1 with $L_1=L_2$

**A. Mode 1  $[t_0-t_1]$ :** As shown in Fig below,  $S_1$  and  $S_3$  are turned on, but  $S_2$  is turned off. Due to  $S_3$  being turned on,  $D_o$  is reverse biased, but  $D_1$  and  $D_2$  are forward biased, thereby causing  $C_e$  to be abruptly charged to  $V_i$  plus  $V_{Cb}$ , whereas due to  $S_1$  being turned on,  $D_b$  is reverse biased, thereby causing  $C_b$  to be discharged. At the same time, the voltages across  $L_1$  and  $L_2$  are  $V_i$  plus  $V_{Cb}$ , thereby causing  $L_1$  and  $L_2$  to be magnetized. Also,  $C_o$  releases energy to the output. In this mode, the voltages across  $L_1$  and  $L_2$ ,  $v_{L1-ON}$  and  $v_{L2-ON}$ , can be written as

$$v_{L1-ON} = V_i + V_{Cb} \quad (3.1)$$

$$v_{L2-ON} = V_i + V_{Cb} \quad (3.2)$$

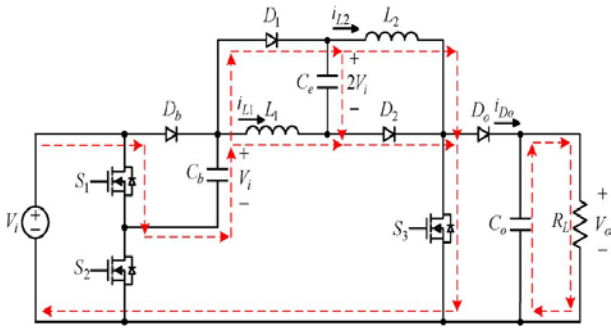


Fig.2 Mode 1

**B. Mode 2  $[t_1-t_2]$ :** As shown in Fig below,  $S_1$  and  $S_3$  are turned off, but  $S_2$  is turned on. Due to  $S_2$  being turned on,  $D_b$  is forward biased, thereby causing  $C_b$  to be abruptly charged to  $V_i$ . At the same time, the input voltage plus the energy stored in  $C_e$  plus the energy stored in  $L_1$  and  $L_2$  supplies the load, thereby causing  $C_o$  to be energized,  $C_e$  to be discharged, and  $L_1$  and  $L_2$  to be demagnetized. By doing so, the output voltage is boosted up, and is much higher than the input voltage. According to the voltage-second balance, the voltages  $v_{L1-OFF}$ ,  $v_{L2-OFF}$ , and  $V_o$  in this mode can be expressed to be

$$v_{L1-OFF} = [-D/(1-D)] * v_{L1-ON} \quad (3.3)$$

$$v_{L2-OFF} = [-D/(1-D)] * v_{L2-ON} \quad (3.4)$$

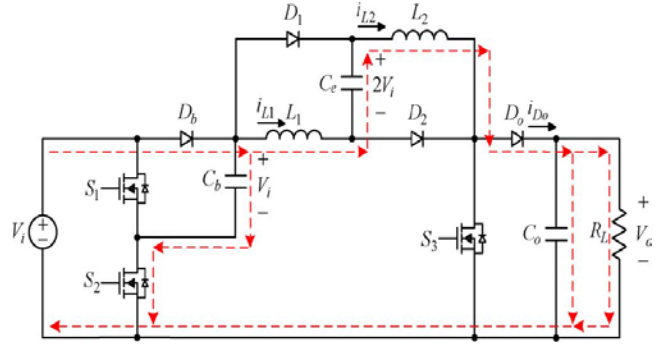


Fig.3 Mode 2

#### 3.1.1 Waveform for Type 1 Converter with $L_1=L_2$

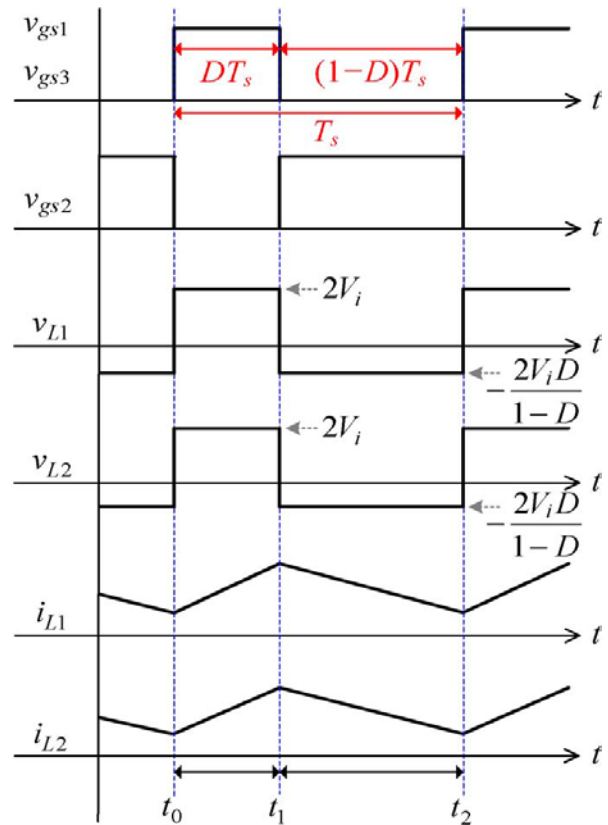


Fig.4 CCM Waveform for type 1 Converter with  $L_1=L_2$

### 3.2 Modes of Operation for Type 2 with $L_1=L_2$

**A. Mode 1  $[t_0-t_1]$ :** As shown in Fig. 3.8,  $S_2$  and  $S_3$  are turned on, but  $S_1$  is turned off. Due to  $S_3$  being turned on,  $D_o$  is reverse biased, but  $D_1$  and  $D_2$  are forward biased, thereby causing  $C_e$  to be abruptly charged to  $V_i$ , whereas due to  $S_2$  being turned on,  $D_b$  is forward biased, thereby causing  $C_b$  to be abruptly

charged to  $V_i$ . At the same time, the voltages across  $L_1$  and  $L_2$  both are  $V_i$ , thereby causing  $L_1$  and  $L_2$  to be magnetized. Also,  $C_o$  releases energy to the output. In this mode, the voltages across  $L_1$  and  $L_2$ ,  $v_{L1-ON}$  and  $v_{L2-ON}$ , can be written as,

$$v_{L1-ON} = V_i \quad (3.8)$$

$$v_{L2-ON} = V_i \quad (3.9)$$

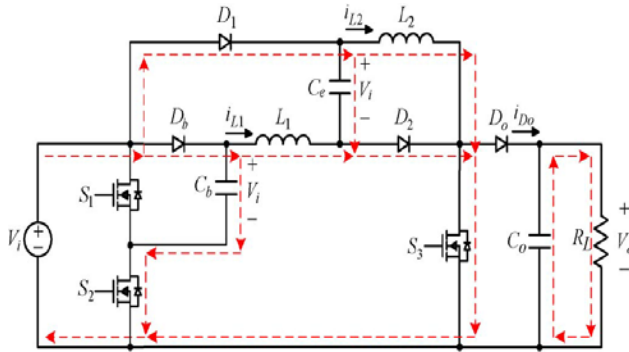


Fig.5 Type 2 mode 1 operation

**B. Mode 2  $[t_1-t_2]$ :** As shown in Fig.3.9,  $S_2$  and  $S_3$  are turned off, but  $S_1$  is turned on. At the same time, the input voltage plus the energy stored in  $C_b$  and  $C_e$  plus the energy stored in  $L_1$  and  $L_2$  supplies the load, thereby causing  $C_o$  to be energized,  $C_b$  and  $C_e$  to be discharged, and  $L_1$  and  $L_2$  to be demagnetized. By doing so, the output voltage is boosted up, and is higher than the input voltage. According to the voltage-second balance, the voltages  $v_{L1-OFF}$ ,  $v_{L2-OFF}$  and  $V_o$  can be expressed as

$$v_{L1-OFF} = [-D/(1-D)] * v_{L1-ON} \quad (3.10)$$

$$v_{L2-OFF} = [-D/(1-D)] * v_{L2-ON} \quad (3.11)$$

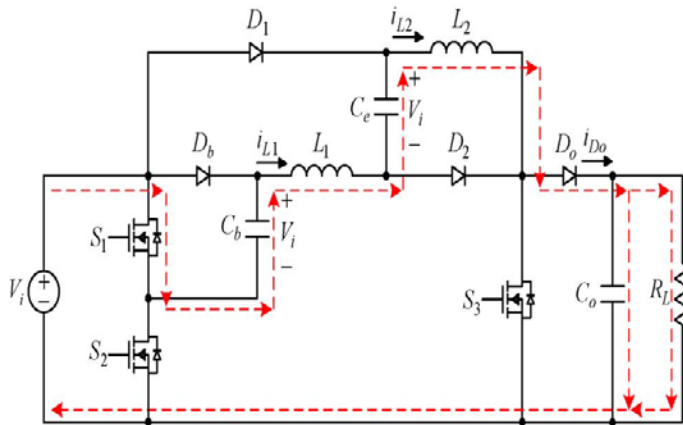


Fig.6 Type 2 Mode 2 Operation

### 3.2.1 Waveforms for Type 2 Converter with $L_1=L_2$

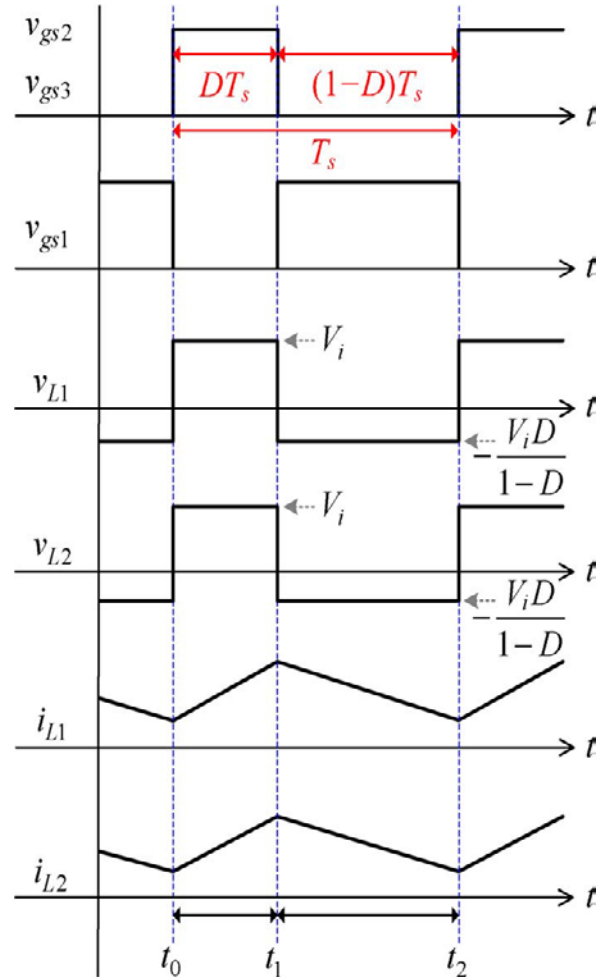


Fig.7 Waveforms for type 2 converter with  $L_1=L_2$

## 4. Simulation and Result Analysis

This chapter gives a review of simulation circuit details of the proposed high voltage converter based on bootstrap capacitors. PI control method is applied to control the duty ratio of switches. Simulation of high voltage DC-DC converter was performed using MATLAB/SIMULINK to confirm analysis explained in previous chapter.

#### 4.1 Open Loop Simulation and Waveforms of High Voltage Boosting Converters

The circuit was drawn in SIMULINK/MATLAB in open loop. The various parameters given according to design as explained earlier in this chapter are shown in Table 1.

Table.1 Simulation Parameters

Parameters	Value
Power rating	100W
Input Voltage	24 V
Switching Frequency	195Khz
Output Voltage	200V
Inductors	170 $\mu$ H
Bootstrap Capacitor, $C_1$	100 $\mu$ F
Output Capacitor, $C_3$	680 $\mu$ F
Load Resistance	400 $\Omega$
Capacitor, $C_2$	220 $\mu$ F

#### 4.2 Open Loop Simulation of Type 1 Converter

The simulation circuit drawn in MATLAB/SIMULINK is shown in Fig 8. The input DC is given using DC voltage supply block. There are three switching MOSFETs in the circuit. Gating pulses are given to the switches using a subsystem. The signals so formed are given to a scope to be verified. The input voltage, output currents, current through the inductors, voltage across the output load is examined.

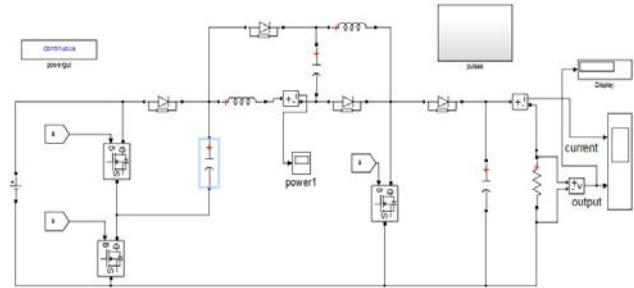


Fig.8 (a) Open loop Circuit for Type1 Converter

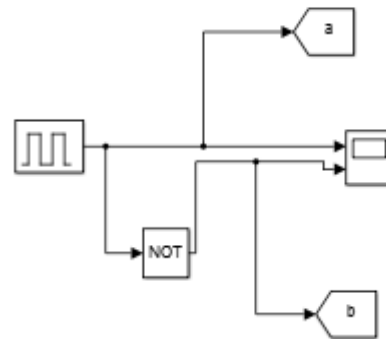


Fig.8 (b) Switching Control Module

#### 4.2.1 Open Loop Simulation Results

The results obtained after the simulation of the converter in open loop circuit are as follows:

##### A. Input Voltage

The input voltage waveform given as shown in Fig 9. In the design consideration, the input voltage was taken to be 24V.

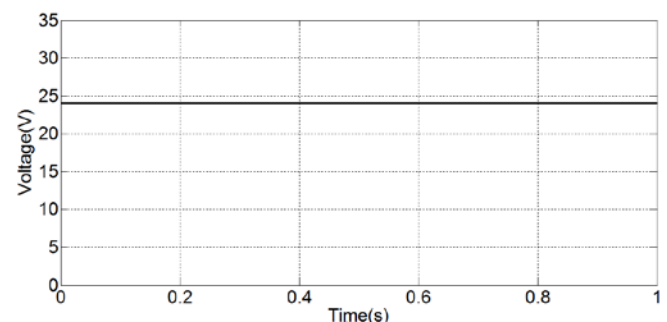


Fig.9 Input Voltage

### B. Output Voltage

The output voltage obtained is as shown below. The output voltage of 207V is obtained and the ripple content in the output voltage is very low. Project aim is fulfilled by achieving a high boosting voltage of 207 V from a 24 V input. The model is simulated by setting duty ratio as 0.65 to achieve this boosting.

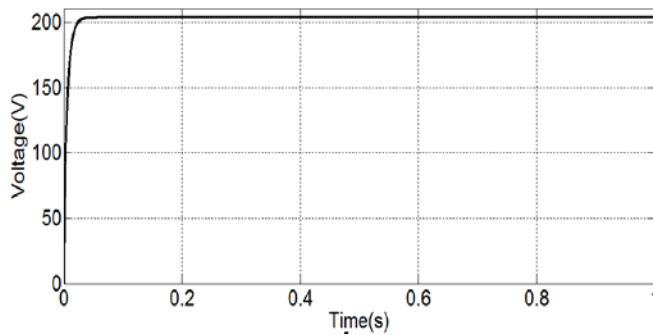


Fig.10 Output Voltage

### C. Inductors Currents with Gate Pulse ( $L_1$ & $L_2$ )

In the design consideration, both the inductors have equal parameters (i.e.  $L_1=L_2$ ), Fig 4.4 shows the inductors' currents along with gate pulses. By analyzing the graphs, it is clear that both inductors are magnetizing and demagnetizing in same manner with respect to the gate pulses. These graphical representations of the current waveforms describe the identical working of two boost inductors in continuous conduction mode.

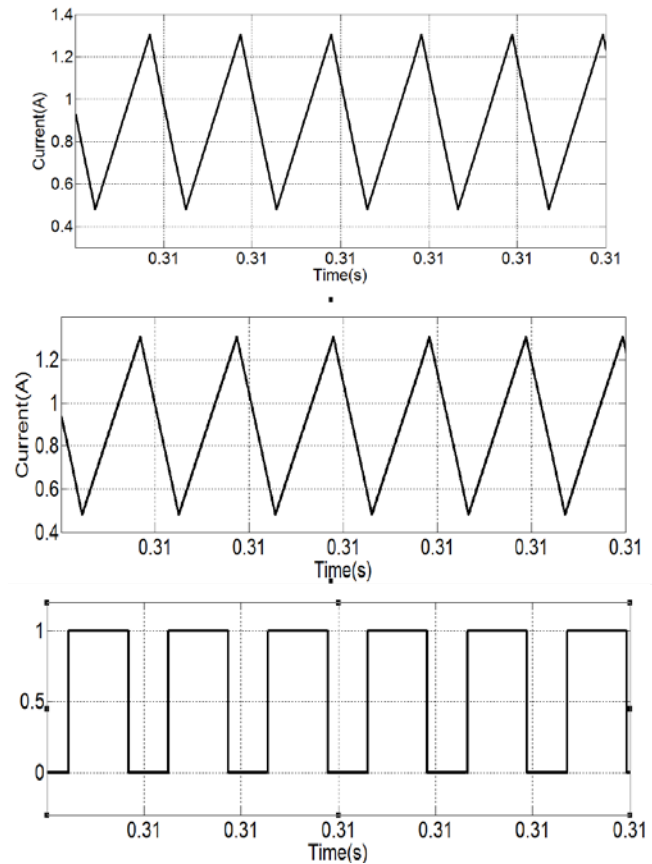


Fig.11 Inductor Currents ( $i_{L1}$  &  $i_{L2}$ ) with Gate Pulse

### 4.2 Open Loop Simulation of Type 2 Converter

The circuit simulated in SIMULINK/MATLAB in open loop. The various parameters given according to design as explained earlier in this chapter are shown in Table 4.3.

Table.2 Simulation Parameters

Parameters	Value
Power rating	100 W
Input Voltage	24 V
Switching Frequency	195 kHz
Output Voltage	145 V
Inductors	80 $\mu$ H

Bootstrap Capacitor, $C_1$	330 $\mu$ F
Output Capacitor, $C_3$	680 $\mu$ F
Load Resistance	400 $\Omega$
Capacitor, $C_2$	330 $\mu$ F

The simulation circuit drawn in MATLAB/SIMULINK is shown in Fig 12. The input DC is given using DC voltage supply block. There are three switching MOSFETs in the circuit. Gating pulses are given to the switches using a subsystem. The signals so formed are given to a scope to be verified. The input voltage, output currents, current through the inductors, voltage across the output load is examined.

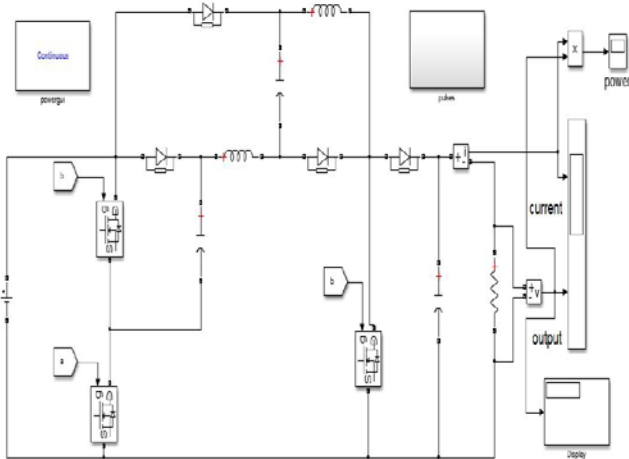


Fig.12 Type 2 converter

#### 4.2.1 Simulation Results

##### A. Input Voltage

The input voltage waveform given as shown. In the design consideration, the input voltage was taken to be 24V.

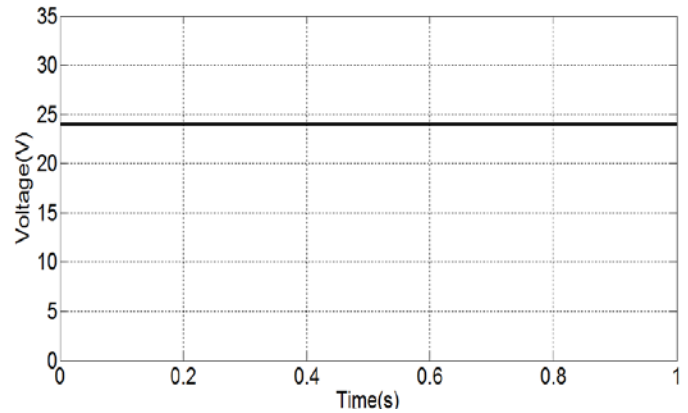


Fig.13 Input voltage

##### B. Output Voltage

The output voltage obtained is as shown below. The output voltage of 166 V is obtained and the ripple content in the output voltage is very low. Project aim is fulfilled by achieving a high boosting voltage of 166 V from a 24 V input. The model is simulated by setting duty ratio as 0.65 to achieve this boosting.

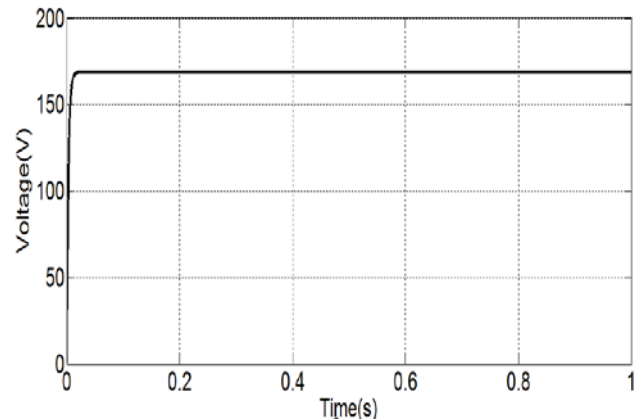


Fig.14 Output voltage

##### C. Output Current

The output current obtained is as shown below. The output current of 1.8A is obtained.

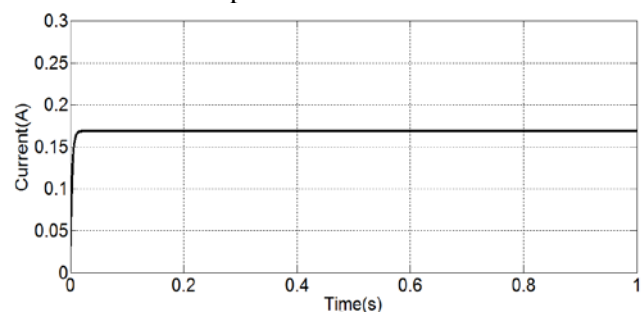


Fig.15 Output current

#### D. Inductors Currents with Gate Pulse ( $L_1$ & $L_2$ )

In the design consideration, both the inductors have equal parameters (i.e.  $L_1=L_2$ ), Fig 4.9 shows the inductors' currents along with gate pulses. By analyzing the graphs, it is clear that both inductors are magnetizing and demagnetizing in same manner with respect to the gate pulses. These graphical representations of the current waveforms describe the identical working of two boost inductors in continuous conduction mode.

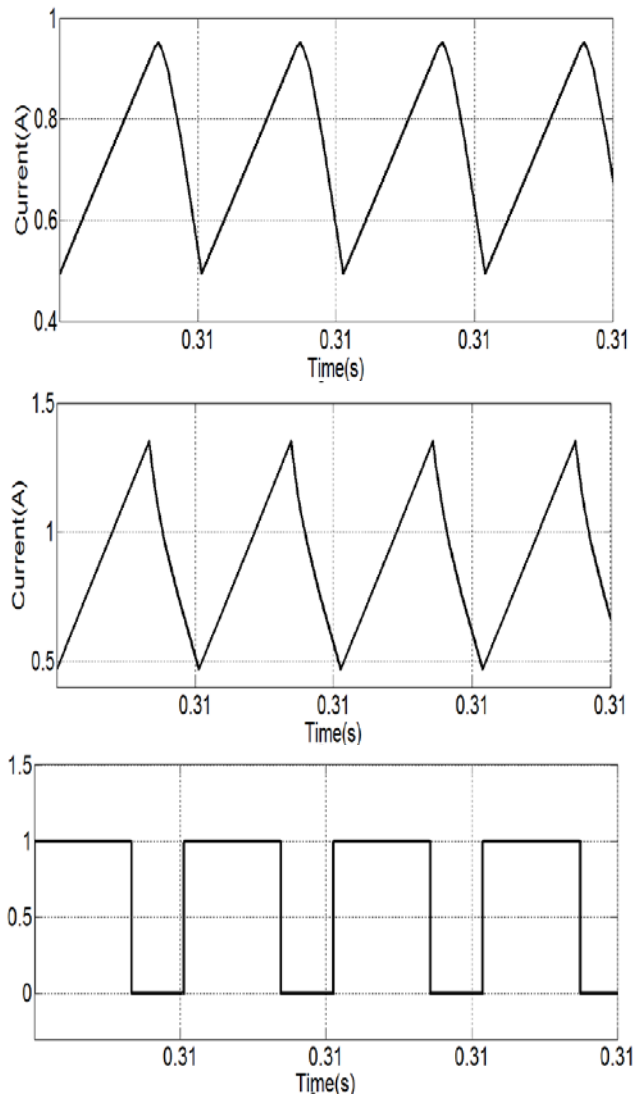


Fig.16 Inductor currents ( $i_{L1}$  &  $i_{L2}$ ) with gate pulse

#### 4.3 Closed Loop Simulation

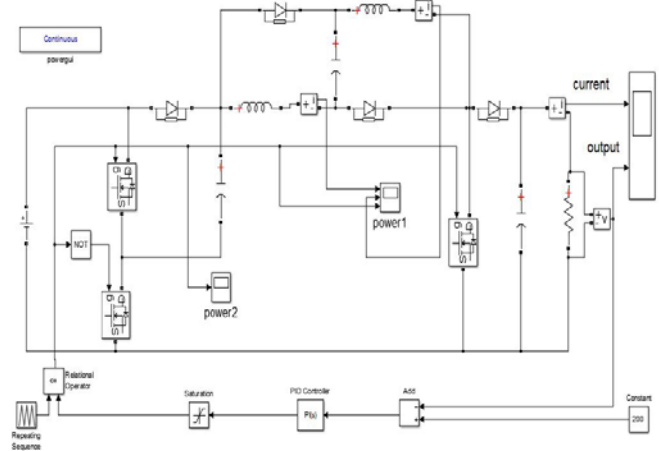


Fig.17 Closed loop simulation

##### 4.3.1 Closed Loop Simulation Results

###### A. Input Voltage

The input voltage waveform given as shown, In the design consideration, the input voltage was taken to be 24V.

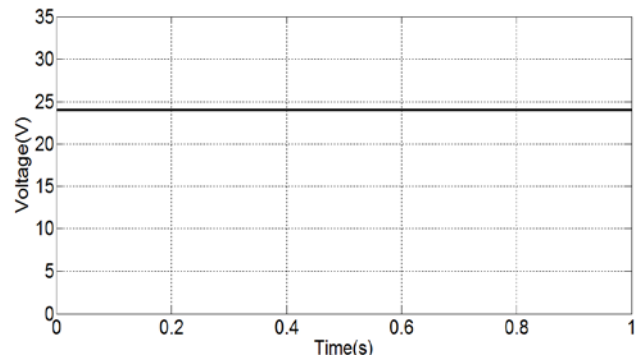


Fig.18 Input voltage

###### B. Output Voltage

The output voltage waveform was obtained as shown, for a 24V DC input voltage, converter output voltage of 200V is obtained and the ripple content in the output voltage is low.

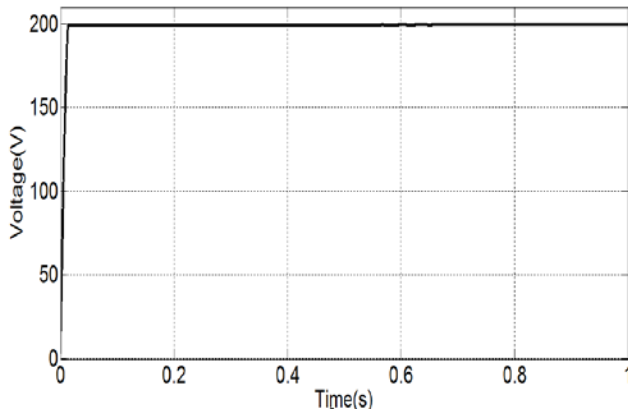


Fig.19 Output voltage

### C. Output Current

The output current obtained is as shown below. The output current of 0.39A is obtained.

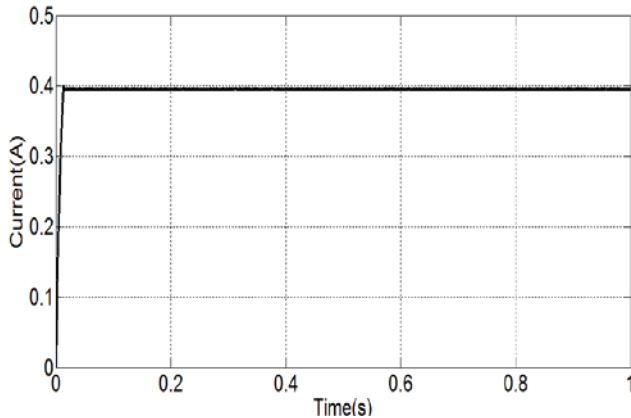


Fig.20 Output current

### D. Inductors Currents with Gate Pulse ( $L_1$ & $L_2$ )

In the design consideration, both the inductors have equal parameters (i.e.  $L_1=L_2$ ), Fig 20 shows the inductors' currents along with gate pulses. By analyzing the graphs, it is clear that both inductors are magnetizing and demagnetizing in same manner with respect to the gate pulses. These graphical representations of the current waveforms describe the identical working of two boost inductors in continuous conduction mode.

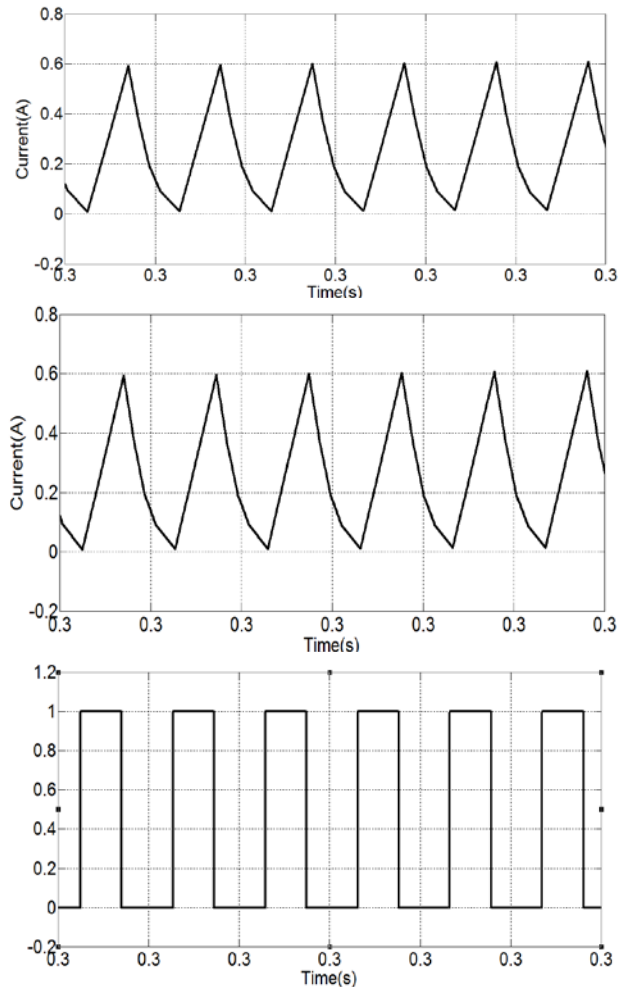


Fig.21 Inductor currents ( $i_{L1}$  &  $i_{L2}$ ) with gate pulse

The simulation of the proposed system is successfully done and explained in this chapter. The simulation results meet all the needs of the proposed system. The open loop simulations for both the converters and closed loop simulation for Type 1 converter are done and waveforms are obtained. By comparing open loop simulations of the both converters, Type 1 converter has better voltage conversion ratio and better performance. Then, next step is to verify the simulation results with the hardware implementation. Next chapter describes the details of hardware implementation and component selection.

## 5. Experimental Setup of the High Voltage Boosting Converter

The simulations of the high voltage boosting converter are successfully done and have been explained in the previous chapter. The simulation

results meet all the needs of the system. Now, next step is to verify the simulation results with the hardware implementation. This chapter describes the details of hardware implementation and component selection.

### 5.1 Hardware Design

The hardware is designed to get a constant well regulated DC as output. In hardware the switching pulse generation is implemented using micro controller unit, dsPIC30F2010. Hardware setup consists of power circuit, control circuit, gate driving circuit and control circuit power supply. The design procedure obtained after the analysis of proposed circuit is used for designing hardware circuit components. The hardware is designed for a lower power and lower voltage converter and the hardware parameters obtained are shown in Table.3.

Table.3 Hardware Parameters

Parameters	Value
Power rating	100 W
Input Voltage	12 V
Switching Frequency	195 kHz
Output Voltage	100 V
Inductors	170 $\mu$ H
Bootstrap Capacitor, $C_1$	100 $\mu$ F, 200 V
MOSFET Driver	TLP250
dsPIC	30F2010, 28PIN
Output Capacitor, $C_3$	680 $\mu$ F, 200 V
Load Resistance	400 $\Omega$
Capacitor, $C_2$	220 $\mu$ F

### 5.2 Experimental Setup



Fig.22 Hardware Experimental Setup

### 5.3 Hardware Results

The hardware results of the proposed system are described. The control part of the hardware circuit is implemented with the help of a microcontroller unit. The circuit is designed to get a well regulated constant DC as output. The output waveforms are viewed with the help of a digital storage oscilloscope.

The input voltage, inductor current, switching pulses and output DC voltage waveforms of hardware implementation are shown below.

#### 5.3.1 Input DC Voltage

In hardware implementation 12 V is used as input DC voltage. Input value and output boosting voltage is reduced proportionally to avoid complexity. So the expected output boosting voltage for an input of 12 volt is 100 V.

#### 5.3.2 Switching Pulses

Fig 23 shows the three gate pulses which are used to switch the three switching devices. The microcontroller control Pulse width modulation pins generate the switching pulses to the gate driver circuit which converts pulses suitable for the switches. in this hardware implementation, three switches are available, but here only need one pulse. Because two switches have identical switching and one switch need its complementary pulse. Here the pulses obtained from the dsPIC are shown.

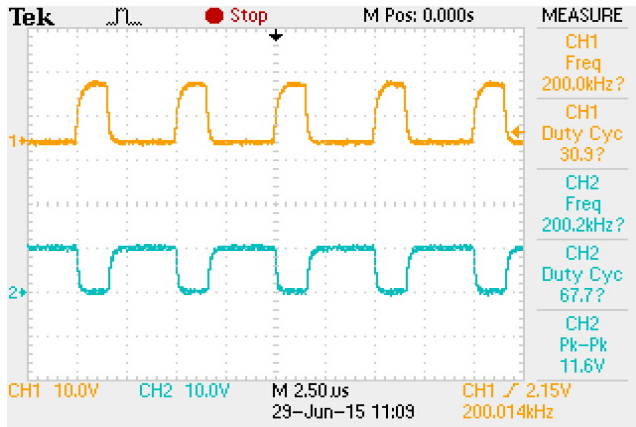


Fig.23 Switching Pulses

### 5.3.3 Inductor Currents ( $L_1$ & $L_2$ )

In the design consideration, both the inductors have equal parameters (i.e.  $L_1 = L_2$ ), Fig 24 shows the inductors' currents along with gate pulses. by analyzing the graphs, it is clear that both inductors are magnetizing and demagnetizing in same manner with respect to the gate pulses. These graphical representations of the current waveforms describe the identical working of two boost inductors in continuous conduction mode.

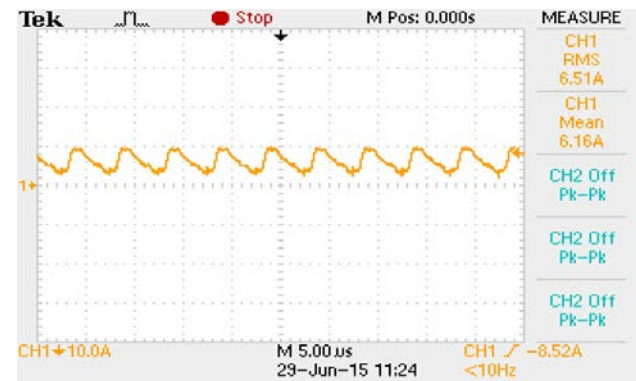


Fig.24 (a) Inductor Current ( $L_1$ )



Fig.24 (b) Inductor Current ( $L_2$ )

### 5.7.4 Output DC Voltage and Output Current

Fig 25 shows the output DC voltage. The objective of the project was a well regulated DC output voltage. The figure shows the output voltage is a regulated one with low ripples. DC output voltage is obtained as 100V and the output current value obtained was 203 mA.

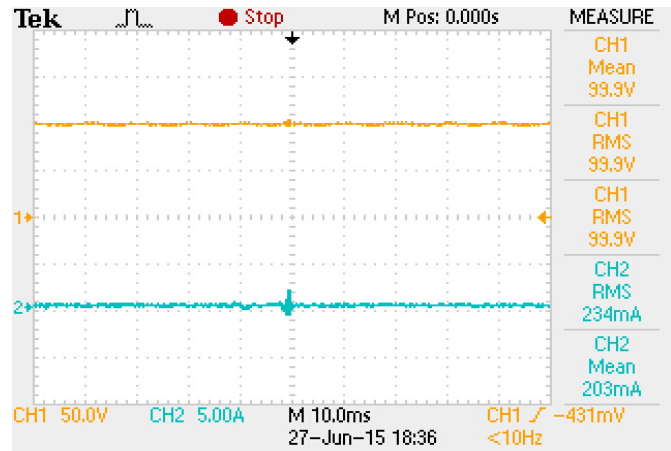


Fig.25 Output DC Voltage and Output Current

The circuit was implemented with power circuit and control circuit on two separate PCBs. The prototype output was obtained from the DSO which is similar to that of the simulation results. These results are analyzed in this chapter.

## 6. Conclusion

In this project work, two high voltage boosting converters were employed. The proposed system was simulated, constructed and functionality of suggested control concept was proven advanced than the prevailing concept. From the detailed simulations an experimental analysis, it is clear that the presented converters have the following advantages.

1. There are two types of high voltage-boosting converters, depending on the circuit connection and the PWM control strategy.
2. The proposed system is simple and easily constructs to achieve expected voltage conversion ratios with fewer losses.
3. For each converter, the power switches are easy to drive, as this converter only needs one PWM

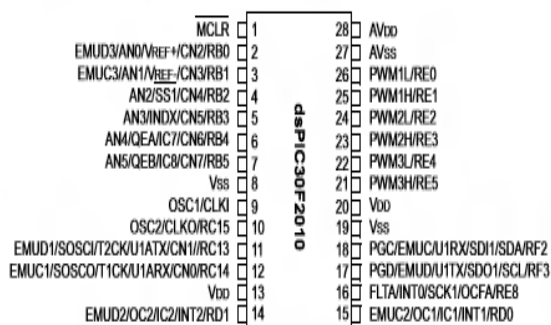
control signal to drive all three switches making its controlling simple.

4. From the experimental results, such converters exhibit good performances even with different inductances, and hence are suitable for industrial applications.

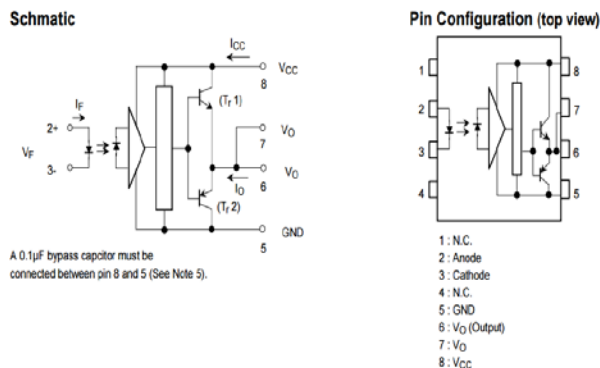
5. Proposed converters need lesser components making it less weight, low cost and compact.

## Appendix

### Pin Diagram of dsPIC30F2010



### TLP250 Schematic diagram and Pin configuration



## Acknowledgments

I am obediently thankful to God Almighty, praise and glory is to Him, for all His uncountable bounties and guidance, without which, this work would have never been a reality.

I thank, **Dr. Mohammed Mubarak**, The Principal, for being the source of inspiration during my course of study.

I am extremely grateful to **Mr. Rajin M. Linus**, Associate Professor and Head of the Department, for his valuable suggestions and encouragement that was a constant source of motivation and inspiration for me during the course of this work.

I express my sincere gratitude to **Mr. Ajmal K. T.**, Assistant Professor and Project Coordinator for his encouragement and for providing all facilities, which helped me to complete this part of project.

I would like to thank my project guide, **Mr. Nayas Qudrathulla P. P.**, Assistant Professor, Department of Electrical and Electronics Engineering, for his valuable guidance and timely support throughout the project work. He has always a constant source of encouragement.

I thank all the staff members of the department for their help and assistance during my project.

My humble gratitude and heartiest thanks also goes to my parents and friends, who have supported and helped me during the course of this work.

## References

- [1] W. Li and X. He, "Review of no-isolated high step-up dc-dc converters in photovoltaic grid-connected applications," *IEEE Trans. Ind. Electron.* vol. 58, no. 4, pp. 1239–1250, Apr. 2011.
- [2] H. Tao, J. L. Duarte, and M. A.M. Hendrix, "Line-interactive UPS using a fuel cell as the primary source," *IEEE Trans. Ind. Electron.*, vol. 55, no. 8, pp. 3012–3021, Aug. 2008.
- [3] D. Nicolae, C. Richards, and J. van Rensburg, "Boost converter with improved transfer ratio," in *Proc. IEEE IPEC, 2010*, pp. 76–81.
- [4] B. Axelrod, Y. Berkovich, and A. Ioinovici, "Switched-capacitor switched-inductor structures for getting transformerless hybrid dc-dc PWM converters," *IEEE Trans. Circuits Syst. I, Reg. Papers*, vol. 55, no. 2, pp. 687–696, Mar. 2008.
- [5] K. I. Hwu and Y. T. Yau, "Voltage-boosting converter based on charge pump and coupling inductor with passive voltage

- clamping," *IEEE Trans. Ind. Electron.*, vol. 57, no. 5, pp. 1719–1727, May 2010.
- [6] K. C. Tseng and T. J. Liang, "Novel high-efficiency step-up converter," *Proc. Inst. Elect. Eng.—Elect. Power Appl.*, vol. 151, no. 2, pp. 182–190, Mar. 2004.
- [7] W. Li and X. He, "A family of isolated interleaved boost and buck converters with winding-cross-coupled inductors," *IEEE Trans. Power Electron.*, vol. 23, no. 6, pp. 3164–3173, Nov. 2008.
- [8] K. B. Park, H. W. Seong, H. S. Sim, G. W. Moon, and M. J. Youn, "Integrated boost-sepic converter for high step-up applications," in *Proc. IEEE PESC, 2008*, pp. 944–950.
- [9] Q. Zhao and F. C. Lee, "High-efficiency, high step-up dc-dc converters," *IEEE Trans.*
- [10] L. S. Yang, T. J. Liang, and J. F. Chen, "Transformerless dc-dc converters with high step-up voltage gain," *IEEE Trans. Ind. Electron.*, vol. 56, no. 8, pp. 3144–3152, Aug. 2009.
- [11] C. E. Silva, R. P. Bascope, and D. S. Oliveira, "Proposal of a new high voltage-boosting converter for UPS application," in *Proc. IEEE ISIE, 2006*, pp. 1288–1292.
- [12] A. A. Fardoun and E. H. Ismail, "Ultra step-up dc-dc converter with reduced switch stress," *IEEE Trans. Ind. Appl.*, vol. 46, no. 5, pp. 2025–2034, Sep./Oct. 2010.
- [13] E. H. Ismail, M. A. Al-Saffar, and A. J. Sabzali, "High conversion ratio dc-dc converters with reduced switch stress," *IEEE Trans. Circuits Syst. I, Reg. Papers*, vol. 55, no. 7, pp. 2139–2151, Aug. 2008.
- [14] E. H. Ismail, M. A. Al-Saffar, A. J. Sabzali, and A. A. Fardoun, "A family of single-switch PWM converters with high voltage-boosting conversion ratio," *IEEE Trans. Circuits Syst. I, Reg. Papers*, vol. 55, no. 4, pp. 1159–1171, May 2008.
- [15] K. I. Hwu and Y. T. Yau, "KY converter and its derivatives," *IEEE Trans. Power Electron.*, vol. 24, no. 1, pp. 128–137, Jan. 2009.
- [16] K. I. Hwu and Y. T. Yau, "A KY boost converter," *IEEE Trans. Power Electron.*, vol. 25, no. 11, pp. 2699–2703, Nov. 2010.
- [17] K. I. Hwu and Y. T. Yau, "High step-up converter based on charge pump and boost
- [18] M. Zhu and F. L. Luo, "Series SEPIC implementing voltage-lift technique for dc-dc power conversion," *IET Power Electron.*, vol. 1, no. 1, pp. 109–121, Mar. 2008.
- [19] Y. He and F. L. Luo, "Analysis of Luo converters with voltage-lift circuit," *Proc. Inst. Elect. Eng.—Elect. Power Appl.*, vol. 152, no. 5, pp. 1239–1252, Sep. 2005.
- [20] M. Cacciato, A. Consoli, and V. Crisafulli, "A high voltage gain dc/dc converter for energy harvesting in single module photovoltaic applications," in *Proc. IEEE ISIE*.

**ASEEB P.P.** received the B.E. degree in electrical engineering from Visvesvarayya Technical University, Belgam, India in 2013 and is currently pursuing the M.Tech degree at M.E.A. Engineering College under Calicut University, Kerala.



**NAYAS QUDRATHULLA P. P** received the B.Tech. degree in electrical engineering from Calicut University, Kerala, India in 2011, received the M.Tech degree in Power Electronics and Drives from Anna University and is currently working as Assistant Professor in M.E.A Engineering College, Perintalmanna.